Journal of Sound and Vibration 327 (2009) 183–196

Contents lists available at ScienceDirect

Journal of Sound and Vibration

journal homepage: www.elsevier.com/locate/jsvi

Experimental identification of nonlinear dynamic properties of built-up structures

L. Heller [a,*], E. Foltête [b], J. Piranda [b]

[a] Institute of Physics ASCR, v.v.i., Na Slovance 2, Prague 18221, Czech Republic
[b] Institute FEMTO-ST, Laboratory of Applied Mechanics, University of Franche-Compté, 25000 Besançon, France

ARTICLE INFO

Article history:
Received 26 October 2007
Received in revised form
30 May 2009
Accepted 2 June 2009
Handling Editor: C.L. Morfey
Available online 28 June 2009

ABSTRACT

The paper is focused on the nonlinear damping capacity of built-up structures owing to presence of frictional joints. To quantify and characterise the nonlinear dynamic behaviour of built-up structures, a novel experimental procedure is introduced based on the wavelet transform providing equivalent modal parameters identification. In order to analyse the influence of the interfacial pressure and the interface area on the dynamic behaviour of built-up structures, an experimental study conducted on a simple built-up structure consisting of two bolted beams is presented. Results in terms of equivalent modal parameters are finally discussed and rationalised.

1. Introduction

Complex mechanical systems are generally composed of simple elements assembled by connections such as bolted, riveted and welded joints. The presence of those mechanical joints affects the dynamic behaviour in terms of eigenfrequency and damping [1,2]. Moreover, the complex transfer behaviour of mechanical joints introduces nonlinearities into the dynamic response of assembled structures. This influence has to be taken into account during the stage of engineering design in order to predict and then optimise the dynamic behaviour. Mechanical joints have also been recognised as one of the main sources of the energy dissipation in complex built-up structures [3,4]. Although this sort of dissipation can be related to many physical phenomena [1], friction between the substructures is considered the most important [2]. The term *slip damping* is used to refer to this mechanism.

The earliest studies of the slip damping were devoted to analysis of simple built-up structures. The joints were idealised by introducing assumptions such as a uniform interfacial pressure [5–7]. Experimental analyses were accompanied by analytical calculations leading to mathematical relations linking the energy dissipation or slip damping to different parameters such as friction coefficient, contact pressure, amplitude of loading, etc. Interesting results coming out of these studies were the existence of an optimal pressure value giving the maximal slip damping [5] and the slip damping dependence proportional to the cube of the loading force amplitude [4].

One of the most important earlier experimental works on slip damping was carried out by Ungar [1]. In his work light assembled structures of the type used in aircrafts were analysed in order to find the origin of the energy dissipation taking place in mechanical joints. The influence of the type of structure and frequency on slip damping was also studied. Ungar proposed a number of semi-empirical equations providing the evaluation of the loss energy factor for some specific structures.

* Corresponding author.
E-mail address: heller@fzu.cz (L. Heller).

0022-460X/$ - see front matter © 2009 Elsevier Ltd. All rights reserved.
doi:10.1016/j.jsv.2009.06.008

More recently, analysis of the slip damping has been oriented to more complex built-up structures. The use of numerical methods such as the finite element method allows to perform complex nonlinear contact analysis giving an insight into the distribution and amount of friction taking place in joints during vibrations. However, these analyses are very difficult to carry out owing to particularly large models that result from a fine discretisation of contact surfaces guaranteeing the numerical stability. Hence, several approaches have been suggested to simplify the numerical analysis of assembled structures. One of the approaches is to apply constitutive models of mechanical joints that use degrees of freedom natural to the scale of structural dynamics. Many constitutive models have been proposed such as Valanis model [8], Iwan model [9,10], Ren's model [11] and the point contact model worked out by Sanliturk and Ewins [12]. The constitutive models are fully defined by a certain number of parameters depending on properties of a given joint. Their determination can be done by using either experimental [9] or numerical approaches [10].

Another way to represent the nonlinear transfer behaviour of mechanical joints is by extending the modal analysis to nonlinear structures. Ferreira and Ewins proposed a method of nonlinear impedance based on the Multi-Harmonic Describing Function [13]. The method consists of taking into account the harmonic oscillations at multiples of the excitation frequency.

The frequency response function (FRF) depending on the excitation amplitude was proposed by Siller [14] who developed a method for detecting, localising, identifying and quantifying the nonlinearities using the amplitude dependent FRF.

Finally, equivalent modal parameters [15] representing the variation of modal parameters with respect to the vibration amplitude has been used [16,17] in order to characterise the dynamical nonlinearities introduced into the system through mechanical joints.

In this paper, we use the equivalent modal parameters to assess the influence of mechanical joints on the dynamic behaviour of assembled structures. First, a mathematical definition of the equivalent modal parameters is introduced for the case of a general mdof system having non-coupled eigenmodes. Then an experimental method for identification of the equivalent modal parameters is proposed. The identification is based on analysis of free-decay responses using the wavelet transform.

The last part of the paper describes an experimental study dealing with a simple built-up structure represented by two overlapped bolted beams. The proposed identification method is applied to analyse the dependence of the equivalent modal parameters on the vibration amplitude, interfacial pressure and surface of the contact area.

2. Definition of equivalent modal parameters

In this paper, we focus on assembled structures consisting of linear substructures. Thus those structures can be considered as dynamic systems locally nonlinear due to the friction in joints. Furthermore, we assume that the friction does not substantially affect the eigenvector linearity. To characterise dynamic systems that meets all these assumptions, the approach of equivalent modal parameters was chosen. According to the well known small-parameter method proposed by Krylov and Bogoljubov [15], the eigenfrequency and modal damping of a locally nonlinear system can be seen as parameters depending on the vibration amplitude. Evolutions of the equivalent modal parameters with respect to the amplitude of vibrations provide information about both the type and the degree of nonlinearities of analysed systems.

The dynamic free motion of a locally nonlinear structure can be approximated by a discrete model whose free dynamic response is defined as a superposition of free motions of N single dof nonlinear oscillators as follows:

$$\mathbf{x} = \mathbf{V}\mathbf{q}, \tag{1}$$

$$x_i = \sum_{j=1}^{N} V_{i,j} a_j(t) \cos \Theta_j(t) = \sum_{j=1} A_j^i(t) \cos \Theta_j(t), \tag{2}$$

where $\mathbf{x}$, $\mathbf{V}$ and $\mathbf{q}$ denote the displacement vector, the modal matrix containing all eigenvectors and the vector of modal coordinates, respectively. A particular modal coordinate q_j is characterised by its amplitude a_j and phase Θ_j.

According to the small-parameter method, the equivalent modal eigenfrequency and damping of N single dof nonlinear modal oscillators are defined by the following set of differential equations:

$$\frac{\mathrm{d}a_j}{\mathrm{d}t} = -\varepsilon_e \zeta_j(a_j)_{n,e} \Omega_j a_j, \tag{3}$$

$$\frac{\mathrm{d}\Theta_j}{\mathrm{d}t} = {}_{d,e}\Omega_j(a_j) = \sqrt{{}_{n,e}\Omega_j(a_j)^2 - \varepsilon^2 ({}_e\zeta_j(a_j)_{n,\mathrm{lin}} \Omega_j)^2}, \tag{4}$$

where the damped eigenfrequency ${}_{d,e}\Omega_j$ and the modal damping ${}_e\zeta_j$ represent the set of equivalent modal parameters and ε denotes the small parameter. As in the case of linear dynamic systems, the equivalent modal damped eigenfrequency is linked to the non-damped equivalent modal eigenfrequency ${}_{n,e}\Omega_i$ and equivalent damping coefficient ${}_e\zeta_i$.

It should be pointed out that the present definition of equivalent modal parameters (Eqs. (3) and (4)) is valid only for systems having non-coupled eigenmodes. In such a case, the contribution of adjacent eigenmodes can be neglected when

systems vibrate at frequencies close to a given eigenmode. Under those assumptions, an experimental method for the equivalent modal parameters identification was developed.

3. Experimental identification of equivalent modal parameters

The proposed experimental method extracts the equivalent modal parameters from the free-decay system response which is assumed to satisfy Eq. (2).

The identification is based on the use of the continues wavelet transform [18,19] which is applied on the free-decay time response. Many experimental studies utilising a wavelet based identification for linear [20–23] and nonlinear systems [24,25] have been published in past two decades. Therefore, only a basic concept of our identification method will be described.

The projection of a free-decay time response provided by the ith accelerometer to the time–frequency domain is defined by the following wavelet transform formula:

$$\mathscr{T}_{x_i}(s,\tau) = \langle x_i(t); \psi_{s,t}\rangle = \frac{1}{\sqrt{s}}\int_{-\infty}^{\infty} x_i(t)\,\overline{\psi\left(\frac{t-\tau}{s}\right)}\,\mathrm{d}t, \tag{5}$$

where s, τ, $\overline{\psi((t-\tau)/s)}$ are the scaling parameter being reciprocally related to the frequency, the time shift and the complex conjugate shifted and scaled mother wavelet function, respectively. The mother wavelet represents a specific function satisfying many mathematical conditions [18,19] such as its well localisation in time and frequency. The choice of a particular mother wavelet is determined by the nature of the time signal to be treated. In our study we deal with oscillating signals being well localised in frequency which implies that the mother wavelet has to be an oscillating function being well localised in frequency. One of the wavelet functions satisfying this requirement is the Morlet function chosen as the mother wavelet for our identification method. The analytical solution of the wavelet transform formula Eq. (5) can be found under the assumption of the asymptotic property of the analysed free-decay response $x_i(t)$. The physical meaning of such a property is that the rate of phase change is much more important than that of amplitude change. If this assumption is satisfied, the free-decay response is projected to the time–frequency domain in the form of a complex 2D function described approximately by the following equation:

$$\mathscr{T}_{x_i}(s,t) \approx \sum_{j=1}^{N} \frac{\sqrt{s}}{2} V_{i,j} a_j(t) \overline{\hat{\psi}(s\,\omega(t))}\,\mathrm{e}^{\mathrm{i}(\Theta_j(t))}, \tag{6}$$

where $\overline{\hat{\psi}(s\omega(t))}$ is the complex conjugate Fourier transform of the wavelet function. The absolute value of complex wavelet transform coefficients can be interpreted as a surface in the time–frequency space as shown in Fig. 1.

The main feature of such a surface is the presence of ridges corresponding to the system eigenfrequencies (Fig. 1). A ridge characterises the variation of a particular eigenfrequency in time that can be considered as an indicator of the stiffness linearity. Such a linearity may be approved by existence of a unique scale value determining the position of the ridge within the entire time interval.

Many algorithms and methods providing the ridge identification and extraction have been proposed [18,19]. The simplest one based on the maximum absolute value of the wavelet transform coefficients is used in our study. Consider a ridge $s_{a,j}(t)$ which corresponds to the jth eigenfrequency. In practical computations, the wavelet transform is calculated only for a discrete vector of scales $s_1 \ldots s_n$. Then the jth ridge laying within a scale interval $s_a \ldots s_b$ is considered to correspond to scales satisfying the following equation:

$$\mathscr{T}_{x_i}(s_{a,j}(t),t) = \max(|\mathscr{T}_{x_i}(s_a \ldots s_b, t)|). \tag{7}$$

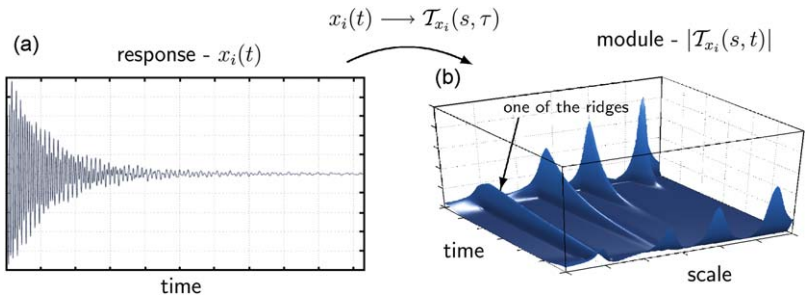

Fig. 1. Example of the time–frequency representation of a free-decay response: (a) time response, (b) module of wavelet transform coefficients.

The jth component of the signal amplitude $A_j^i(t)$ and phase $\Theta_j(t)$ identified at the ith accelerometer can be reconstructed using the wavelet coefficients corresponding to the ridge scales by applying the following equations:

$$A_j^i(t) = \frac{2}{\sqrt{s_{a,j}(t)}} |\mathscr{T}_{x_i}(s_{a,j}(t), t)|, \tag{8}$$

$$\Theta_j(t) = \frac{2}{\sqrt{s_{a,j}(t)}} \arg(\mathscr{T}_{x_i}(s_{a,j}(t), t)). \tag{9}$$

The introduction of Eqs. (8) and (9) into Eqs. (3) and (4) leads to Eqs. (10) and (11) showing that the equivalent modal damping is linked to the logarithm of the module of wavelet coefficients and the equivalent damped eigenfrequency is related to the argument of these coefficients:

$${}_e\zeta_j{}^i(t) = -\frac{1}{n,\mathrm{lin}\Omega_j} \frac{\mathrm{d}\ \ln\left(\frac{2}{\sqrt{s_{a,j}(t)}} |\mathscr{T}_{x,i}(s_{a,j}(t), t)|\right)}{\mathrm{d}t}, \quad j = 1, 2, \ldots, N, \tag{10}$$

$${}_{d,e}\Omega_j{}^i(t) = \frac{\mathrm{d}\ \arg(\mathscr{T}_{x_i}(s_{a,j}(t), t))}{\mathrm{d}t}, \quad j = 1, 2, \ldots, N. \tag{11}$$

Note that the computation of Eqs. (10) and (11) requires the use of a numerical derivation scheme being a very sensitive operation when it is applied on standard measured signals containing a certain level of noise. Therefore, the derivative was computed using the Savitzky–Golay FIR (Finite Impulse Response) smoothing filter.

The time evolution of equivalent modal parameters can be converted to corresponding amplitude dependencies by using the time variation of amplitude $A_j^i(t)$ evaluated by Eq. (8). When several free-decay responses $x_i, i = 1, \ldots, k$, from different places of the structure are provided, the proposed experimental method allows to identify non-normalised eigenvectors. They are related to both the ratio of the absolute value of the wavelet ridge coefficients and their relative phase shifts. Consider two free-decay responses x_i, x_k and the ridge scales $s_{a,j}$ corresponding to the jth eigenfrequency. Then the kth component of the jth non-normalised eigenvector is calculated by the following formulas:

$$|\alpha_{k,j}(t)| = \left|\frac{\mathscr{T}_{x_k}(s_{a_j}, t)}{\mathscr{T}_{x_i}(s_{a_j}, t)}\right|, \tag{12}$$

$$\arg(\mathscr{T}_{x_k}(s_{a_j}, t)) - \arg(\mathscr{T}_{x_i}(s_{a_j}, t)) = 0 \rightarrow \alpha_{k,j}(t) = |\alpha_{k,j}(t)|, \tag{13}$$

$$\arg(\mathscr{T}_{x_k}(s_{a_j}, t)) - \arg(\mathscr{T}_{x_i}(s_{a_j}, t)) = \pm\pi \rightarrow \alpha_{k,j}(t) = -|\alpha_{k,j}(t)|. \tag{14}$$

After having normalised those eigenvectors they can be assembled into the modal matrix $V_{i,j}(t)$ which may be used to calculate the eigenmode amplitude $a_j(t)$ as follows:

$$a_j(t) = A_j^i(t)/V_{i,j}(t). \tag{15}$$

Finally, all the equivalent modal parameters identified on each accelerometer can be evaluated as functions of the eigenmode amplitude (Eqs. (16) and (18)):

$${}_e\zeta_j{}^i(t) \longrightarrow {}_e\zeta_j{}^i(a_j(t)), \tag{16}$$

$${}_{d,e}\Omega_j{}^i(t) \longrightarrow {}_{d,e}\Omega_j{}^i(a_j(t)), \tag{17}$$

$$V_{i,j}(t) \longrightarrow V_{i,j}(a_j(t)). \tag{18}$$

The identified equivalent modal eigenmodes allow for a verification of the assumption of quasi-constant eigenmodes that represents the basic hypothesis the proposed identification method relies on. Furthermore, the identification can be approved by comparing the equivalent modal parameters identified on different accelerometers that should be theoretically identical. Thus those experimentally identified parameters are required to be equal within admissible identification error tolerances $\Delta\zeta$, $\Delta\Omega$ as expressed by

$${}_e\zeta_j{}^i(a_j(t)) = {}_e\zeta_j{}^k(a_j(t)) \pm \Delta\zeta = {}_e\zeta_j(a_j(t)) \pm \Delta\zeta \quad \forall i, k, \tag{19}$$

$${}_{d,e}\Omega_j{}^i(a_j(t)) = {}_{d,e}\Omega_j{}^k(a_j(t)) \pm \Delta\Omega = {}_{d,e}\Omega_j(a_j(t)) \pm \Delta\Omega \quad \forall i, k. \tag{20}$$

4. Experimental investigation of a simple built-up structure

A simple built-up structure with an isolated frictional joint was analysed by using the previously presented experimental identification method. As it has been mentioned, the interfacial pressure and the interface area are the crucial factors determining the final impact of the frictional joint on the dynamic behaviour of the whole structure. Therefore, the experiment was conducted in a way allowing to control those two parameters in order to study their influence on the evolution of equivalent modal parameters.

4.1. Experimental set-up

The analysed structure consisted of two steel beams of dimensions $700 \times 50 \times 15$ mm and $700 \times 50 \times 5$ mm. The beams were assembled by means of three bolts M6 distributed along the beams length. A tube equipped with a strain gauge was inserted between the head of the bolt and the beam (Fig. 2) in order to provide the measurement of the axial force in bolts. Although the axial force gives only an indirect information about the interfacial pressure, the term prestress will be used in the following text to refer to axial force values measured by the strain gauges.

Four different beam assemblages were tested to evaluate the effect of the interface area:

- direct assemblage of two beams (assemblage w0);
- washers inserted between the beams at bolt axes;
  - small washer with an outer diameter of 8 mm (assemblage w1);
  - intermediate washer with an outer diameter of 12 mm (assemblage w2);
  - large washer with an outer diameter of 16 mm (assemblage w3).

In order to simulate free-free boundary conditions, the structure was suspended by means of two wires connected to one of the beams at approximately calculated node positions of the first bending eigenmode. The experimental configuration including measurement equipment is shown in Fig. 2. Although the identification method was based on analysis of free-decay dynamic responses, an electromagnetic shaker was used for the dynamic excitation located at the extremity of the beams where a force transducer and a piezoelectric accelerometer were also placed. Four other accelerometers were distributed along the beam length allowing the eigenmode identification. The use of the electromagnetic shaker for excitation purposes instead of e.g. hammer allowed to enlarge the amplitude interval within which the equivalent modal parameters were identified by using the presented identification method. It was achieved by using a sinusoidal excitation at a frequency close to the desired one that emphasised the presence of the particular eigenfrequency in the response spectrum. The free-decay system response was then obtained by using a system disconnecting the shaker from the structure. This system was realised by means of an electromagnet attached to the bar of the shaker and connecting the force transducer and accelerometer that were both fixed on the structure. An electromagnet power supply control system linked to the data acquisition system was used for synchronising the time of disconnection with the start of the data acquisition.

The complete measurement set-up scheme showing all acquired data is depicted in Fig. 3. Note that an indirect measurement of the interfacial pressure variation during the vibration was allowed by acquiring the strain gauge signals during vibrations.

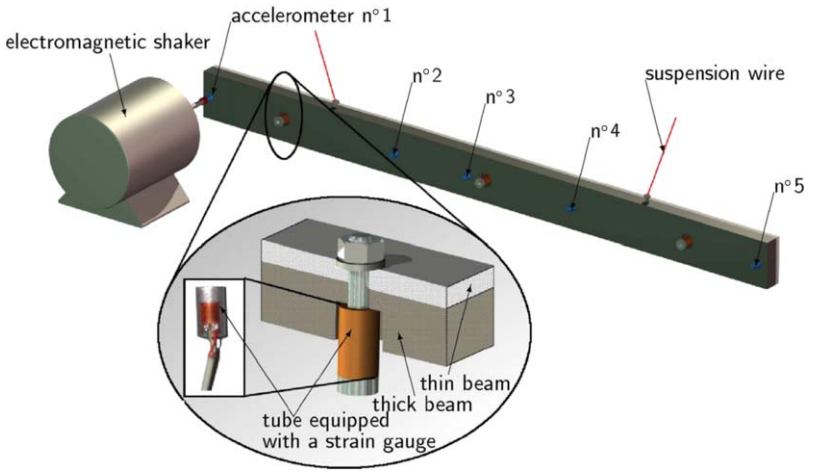

Fig. 2. Experimental set-up and design of two assembled beams.

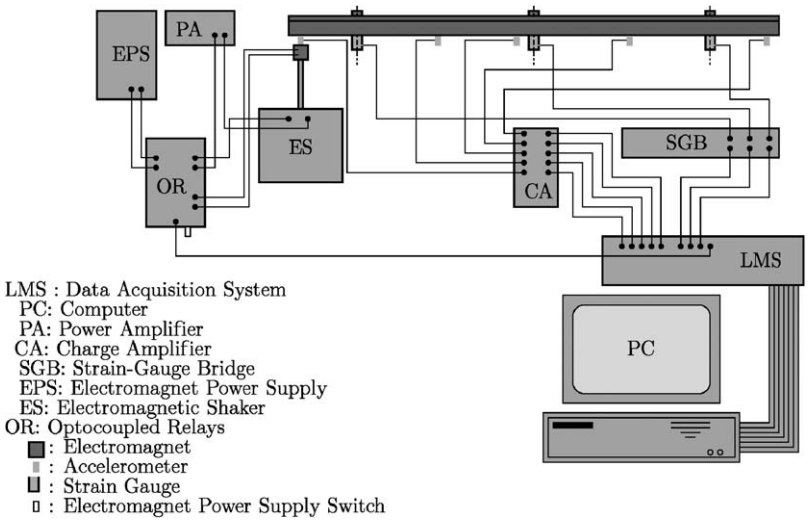

Fig. 3. Experimental set-up scheme with all measurement equipments.

4.2. Measurement technique

The experiment on the assembled beams was focused on the identification of equivalent modal parameters corresponding to the first bending mode. The measurement procedure used for such an identification consisted of two main steps. First, the structure was excited by a harmonic signal at a frequency close to that of the first eigenmode and then the free-decay response was recorded after the shaker disconnection from the structure by using the system described above. The second step consisted of applying the proposed wavelet based equivalent modal parameters identification on the recorded free-decay responses. The overall identification technique comprised the following identification steps:

- computation of the global wavelet transform using a large frequency band;
- localisation of the ridge corresponding to the first eigenfrequency;
- computation of the local wavelet transform using a narrow frequency band around the localised eigenfrequency;
- identification of the first eigenfrequency ridge;
- computation of the time evolution of equivalent modal parameters by using the wavelet transform coefficients corresponding to the first eigenfrequency ridge;
- filtering of the free-decay response for obtaining the first eigenmode component, this step was performed by a pseudo-inverse wavelet transform which is the standard inverse wavelet transform that uses only those wavelet coefficients that correspond to the first eigenfrequency ridge;
- conversion of the filtered acceleration response to displacement, this step allowed the conversion from the time dependencies of equivalent modal parameters to their variations with respect to the displacement amplitude.

4.3. Preliminary modal analysis

First, a preliminary modal analysis using a random noise excitation technique was carried out in order to identify the first bending mode and analyse the influence of prestress on the FRF. Fig. 4 shows a shift of the first eigenfrequency towards higher values when increasing the prestress. Such an effect indicates an increasing stiffness of the assembled structure. Furthermore, the half-power bandwidth decreases when increasing the prestress. Moreover, the FRFs of different assemblages measured at a same applied axial force of 500 N (Fig. 5) show considerable differences in damping expressed by a varying half-power bandwidth. The beams in direct contact display a much higher value of damping than that identified in the case of assemblages with inserted washers. Although the FRFs of beams with inserted washers of different sizes reveal only small changes in the half-power bandwidth, the damping clearly increases with increasing washer size. Hence, as the prestress and the interface area influence the amount of the relative motion between two beams, the experimental results suggest that changes in the friction taking place at the frictional joint are the main cause of observed variations in the equivalent modal parameters.

4.4. Eigenmode nonlinearity

In order to evaluate the impact of the interface area on the eigenvector linearity, a linear finite element model of the assemblage without washers was prepared (Fig. 6) so that the coincident interfacial nodes of two beams were fixed one to

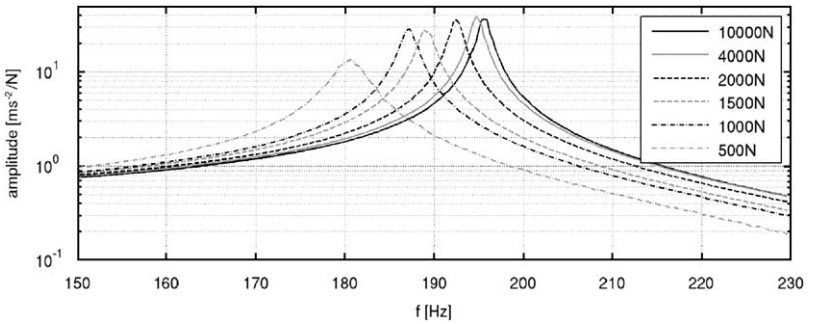

Fig. 4. FRFs measured on beams in direct contact tightened by different bolt axial forces.

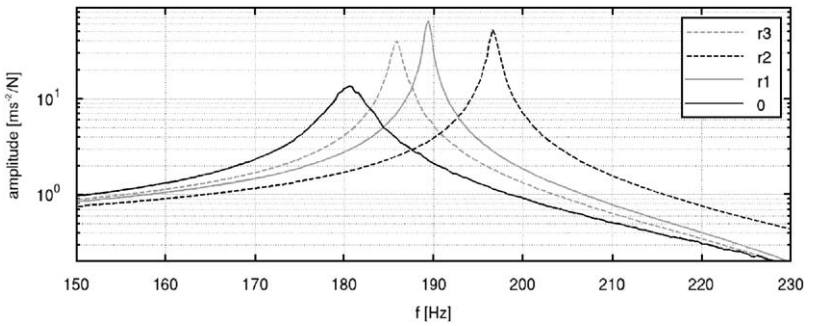

Fig. 5. FRFs obtained on all tested assemblages tightened by an axial force of 500 N.

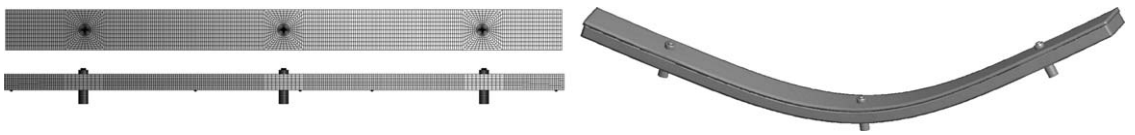

Fig. 6. The finite element mesh of a linearised FEM model and the calculated first eigenmode.

the other i.e. the friction and contact were not considered in the computation. The first bending mode shown in Fig. 6 was then compared to that identified experimentally with respect to the vibration amplitude as it has been explained above.

Figs. 7 and 8 show a comparison between the calculated eigenmode and the mean value of the measured one both expressed in the normalised form. The comparison showing a relative error never exceeding 16 percent proves that the frictional interface of the bolted joint has only a slight influence on the shape of the first eigenvector. Nevertheless, the error distribution along the beam length is not symmetric which might suggest a slight deviation from the eigenmode symmetry due to the frictional joint. Then the normalised experimentally identified eigenvector $V_{i,1}(t),\ i=1,\ldots,5$, was used to convert the identified vibration amplitudes $A_1^i,\ i=1,\ldots,5$, from all accelerometers to the eigenmode amplitude $a_1(t)\ (\equiv a(t))$ as discussed in Section 3 so that we could express all identified modal parameters with respect to the eigenmode amplitude.

After having identified the eigenmode amplitude, the experimental identification of equivalent modal parameters was approved by comparing data from measurements on different accelerometers that were supposed to give the same results within an identification error tolerance as expressed by Eqs. (19) and (20). The identified results satisfied this condition in all measured configurations, an example of this agreement is depicted in Fig. 9 showing the results for an axial force of 5000 N and an assemblage of type w0.

As explained previously, the proposed experimental identification of equivalent modal parameters is developed under the assumption of an eigenmode quasilinearity. Thus to verify such a linearity, the amplitude dependence of the relative deviation of eigenvector components $\Delta_r V_{i,1}(a(t))$ from their values at the minimal vibration amplitude was evaluated using the following equation:

$$\Delta_r V_{i,1}(a(t)) = \frac{V_{i,1}(a(t)) - V_{i,1}(a_{\min})}{|V_{i,1}(a_{\min})|}, \tag{21}$$

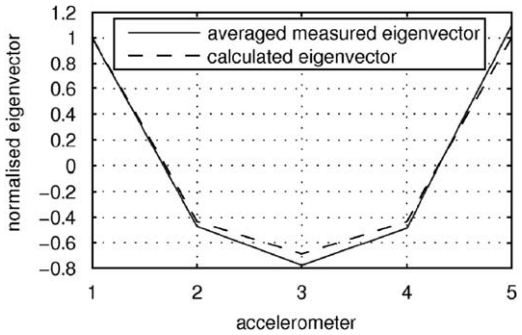

Fig. 7. Comparison of the first eigenmode obtained by FE analysis and measurement.

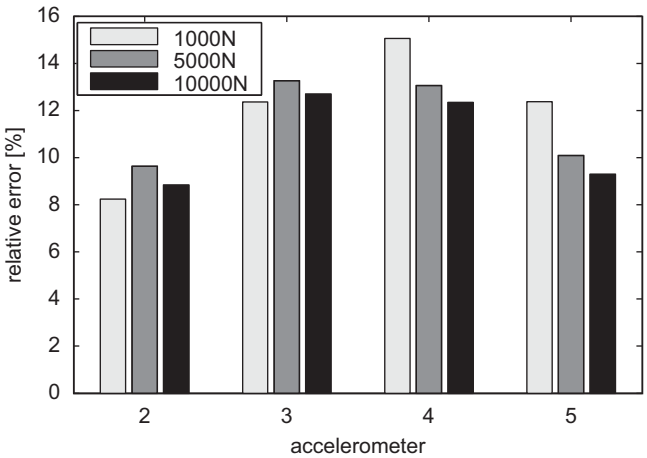

Fig. 8. Relative error between the calculated and the averaged experimentally obtained the first eigenmode.

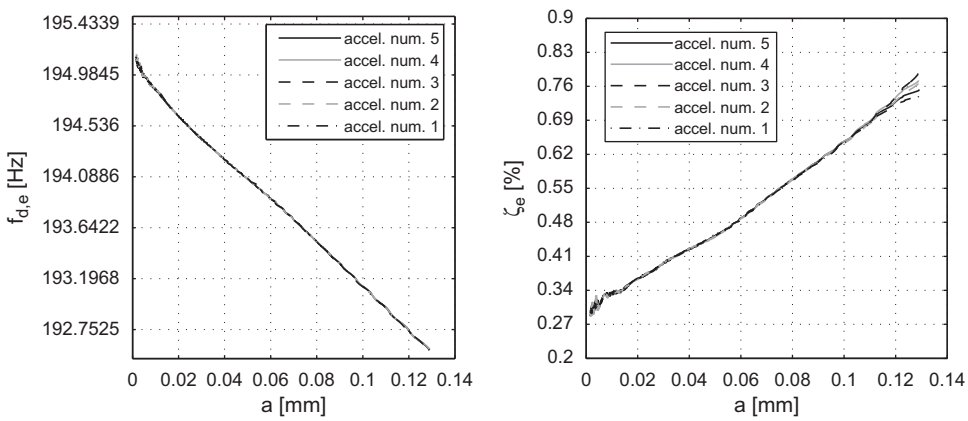

Fig. 9. Comparison of equivalent modal parameters identified on different accelerometers.

where $V_{i,1}(a_{\min})$ denotes the value of the ith component of the first eigenvector at the minimal vibration amplitude reached within free vibrations, whereas $V_{i,1}(a(t))$ represents its instantaneous value.

The evolution of the relative deviation of the third component of the first eigenvector component is shown in Fig. 10 as a representative example. The recorded data were affected by the presence of signal noise (see markers in Fig. 10 representing data points) and therefore a curve fitting was applied on the measured values (solid lines in Fig. 10) to highlight the trend of plotted evolutions. In the case of a linear system no amplitude dependence of eigenvectors exists which would correspond to dashed line in Fig. 10. In contrast, the present dynamic system clearly shows an amplitude

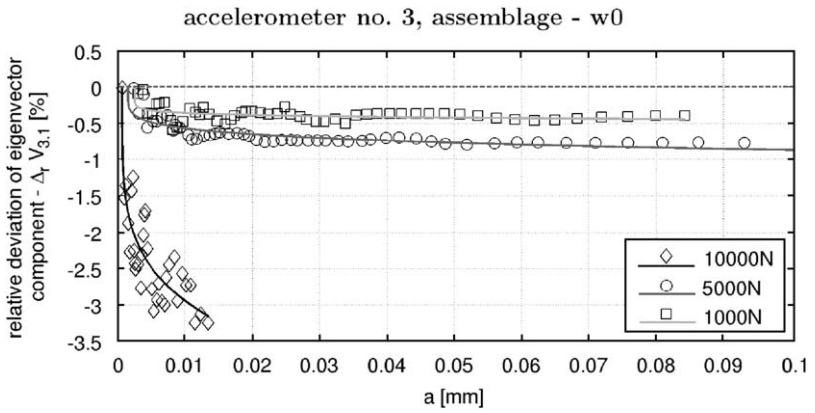

Fig. 10. Amplitude dependence of the relative deviation of the third component of the first eigenvector from its value reached at the minimal vibration amplitude. The dashed line indicates the evolution in the case of an ideal linear system.

dependence of the measured eigenvector. This dependence becomes more important with decreasing prestress that might be interpreted as increasing eigenmode nonlinearity when the role of friction in the dynamic behaviour of the system becomes more important. In the case of higher prestresses (10 000 and 5000 N) only a slight maximum absolute value of the relative deviation of the eigenvector component was identified (<1) percent that was reached already at small amplitudes and did not increase further. However, in the case of a very low prestress (1000 N) the effect of friction on the eigenvector amplitude dependence seems to be more important as the absolute value of the relative deviation shows a higher value ($\sim$3.5) percent and an increasing tendency with increasing amplitude. Nevertheless, as the identified relative deviation of the eigenvector components is limited to few percents, the assumption of the eigenmode quasilinearity seems to be satisfied in the case of the analysed dynamic system.

The eigenvectors could also be affected by a modal coupling due to the nonlinear damping forces. Nevertheless, the very small relative errors indicate that this coupling did not occur, although the orthogonality of the eigenmodes was not verified.

A negligible eigenvector variation with respect to the amplitude and prestress justifies the use of the proposed identification method relying on the Single Degree of Freedom approach. In that situation, a single sensor located anywhere on the structure except on a nodal line allows the identification of the modal equivalent parameters. It is clear that this approach would no longer be valid in the case of a modal coupling due to the nonlinear damping forces. In that case, a Multi-Degree of Freedom technique would be necessary and the questions of the number and locations of sensors would have to be addressed.

4.5. Evolution of equivalent eigenfrequency

As each of studied assemblages has a slightly different geometry, the identified damped eigenfrequencies do not lie at the same frequency level (Fig. 11). However, all assemblages exhibit a nearly linear decrease of the eigenfrequency when increasing the vibration amplitude. The slope of such a decrease depends on the assemblage type i.e. on the interface area. This would suggest that the amplitude dependence of the eigenfrequency can be attributed to the friction at the interface.

The nonlinearity degree of the damped eigenfrequency expressed by the slope of its amplitude dependence dramatically changes when decreasing the axial force as can be seen in Fig. 12. It may be explained by the fact that slightly tightened bolts allow for an important friction motion giving rise to the slip damping that increases with increasing amplitude of vibrations. Consequently, such a vibration amplitude sensitivity of the slip damping is directly projected to the amplitude evolution of the damped eigenfrequency through their relation given by Eq. (4). As the applied prestress increases, the damped eigenfrequency becomes almost constant due to a restricted friction at the interface that limits the role of the slip damping. This stabilisation or linearisation of the eigenfrequency is better represented by the prestress dependence of the eigenfrequency for different amplitude levels as depicted in Fig. 13 which shows data corresponding to the assemblage w0 (no washer inserted). The damped eigenfrequency asymptotically tends to a same limit value for all amplitudes of vibration. Such a limit value can be considered as the eigenfrequency of a corresponding virtual linear system being free of friction.

4.6. Evolution of equivalent damping

The identified equivalent damping showed in Fig. 14 reveals a clear relation between the interface area and the damping level. It increases with increasing interface area for all applied prestresses at a given vibration amplitude. The equivalent damping of the assemblage w0 having beams in direct contact was found to be several times higher than in the case of

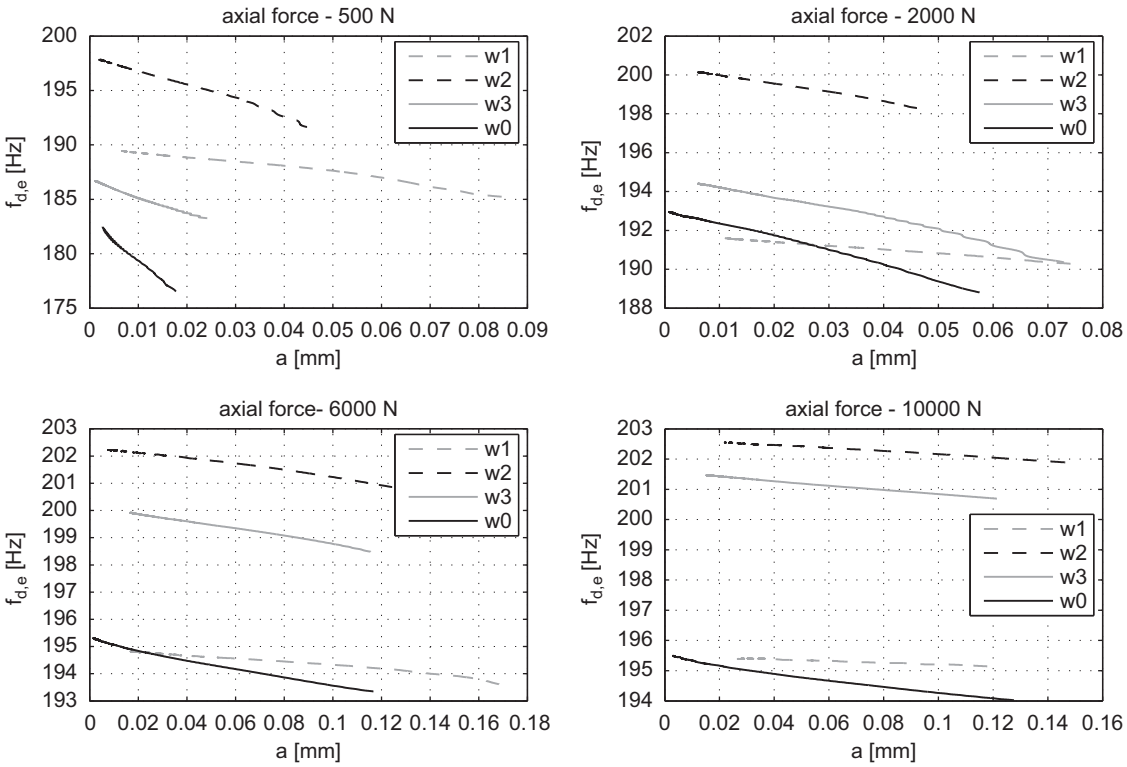

Fig. 11. Effect of the interface area on the vibration amplitude evolution of the damped eigenfrequency at different applied prestresses.

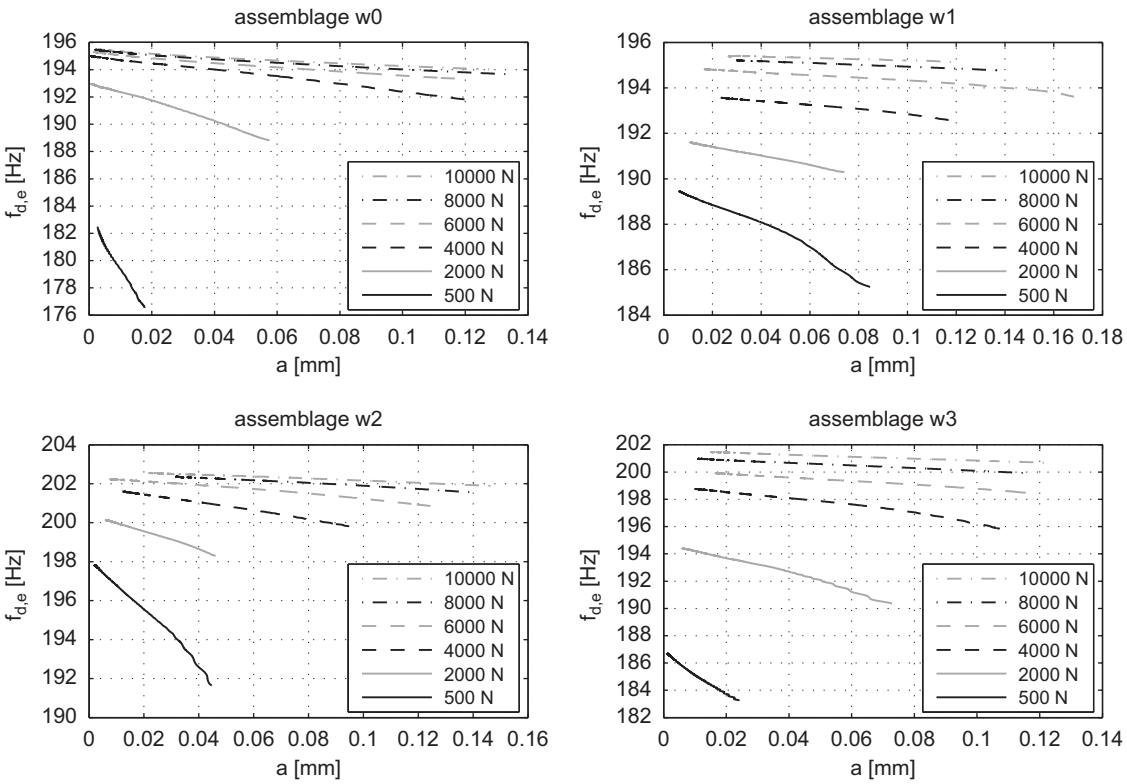

Fig. 12. Effect of the axial bolt force on the vibration amplitude evolution of the damped eigenfrequency corresponding to different assemblage types.

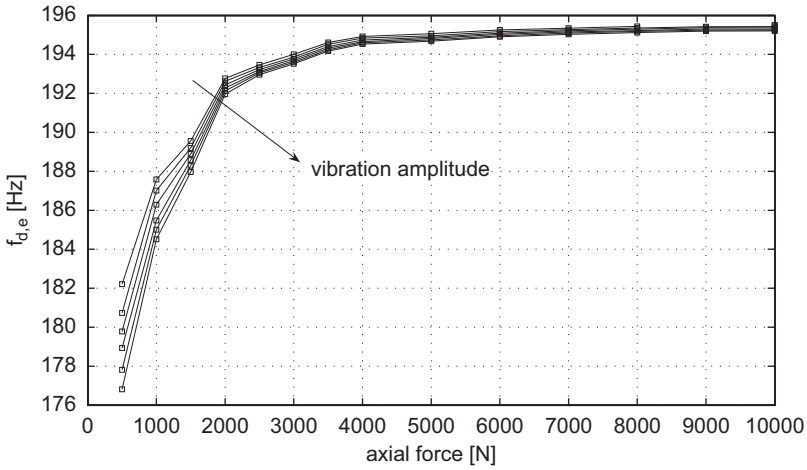

Fig. 13. Asymptotic evolution of the damped eigenfrequency with increasing prestress.

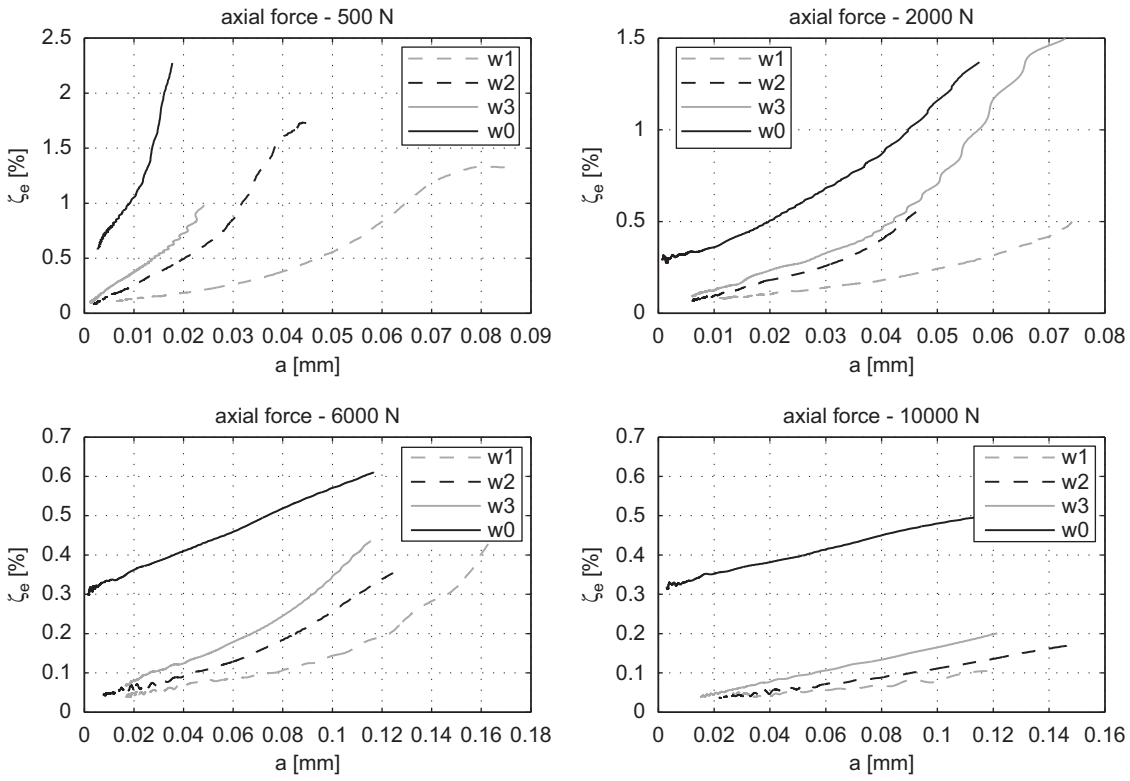

Fig. 14. Effect of the interface area on the vibration amplitude evolution of the equivalent damping coefficient at different applied prestresses.

assemblages with inserted washers. It would suggest that the slip damping plays an important role in the overall energy dissipation of the structure and that the area where an important friction occurs is not limited to a small perimeter around the bolt but is larger than the diameter of the largest washer ($d = 16$ mm).

Fig. 15 also shows an important effect the prestress has on the character of the equivalent damping variation with respect to the vibration amplitude. The equivalent damping variation corresponding to lower prestresses seems to satisfy a power law while a linear evolution is observed in the case of higher prestresses. Moreover, at low prestresses, the assemblages with inserted washers show damping variations satisfying a power law and a local maximum at higher amplitude seems to exist. It could be explained by the existence of a limited perimeter around the bolt axis beyond which the interfacial pressure vanishes. Hence, when the friction area reaches this limit upon increasing vibration amplitude, any further amplitude increase is not accompanied by a damping increase. This local maxima in the equivalent damping

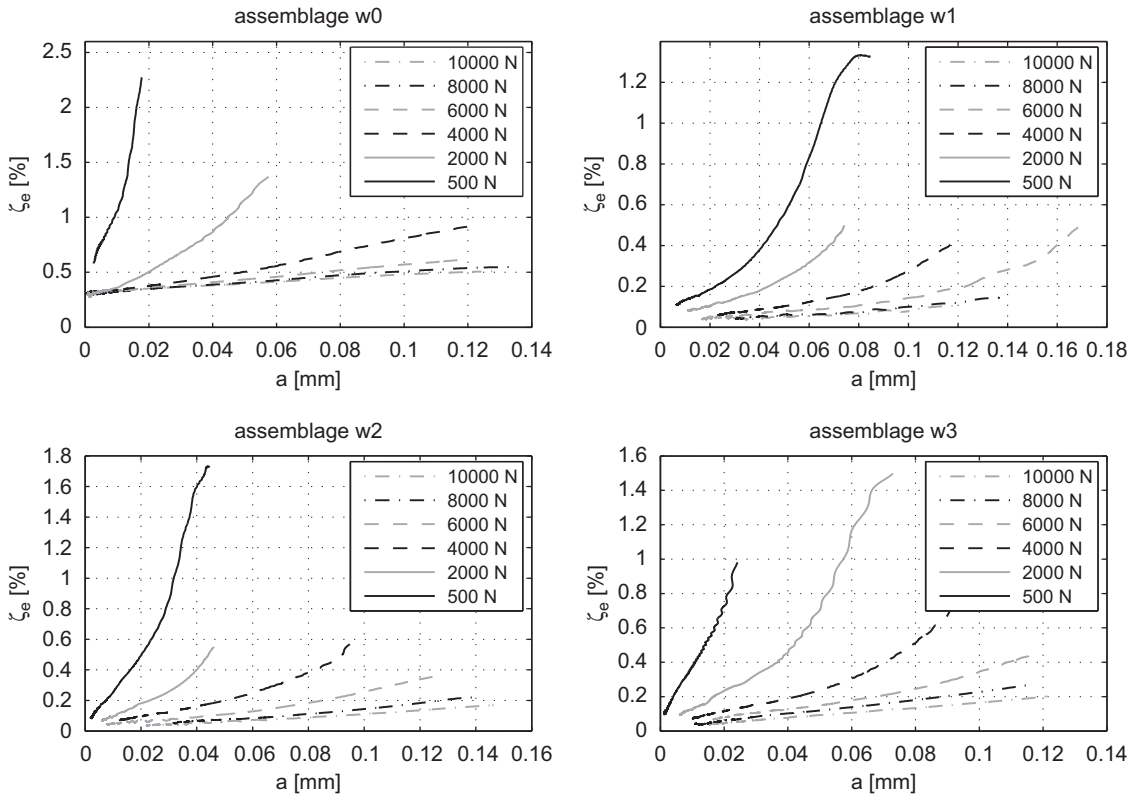

Fig. 15. Effect of the axial bolt force on the vibration amplitude evolution of the equivalent damping coefficient corresponding to different assemblage types.

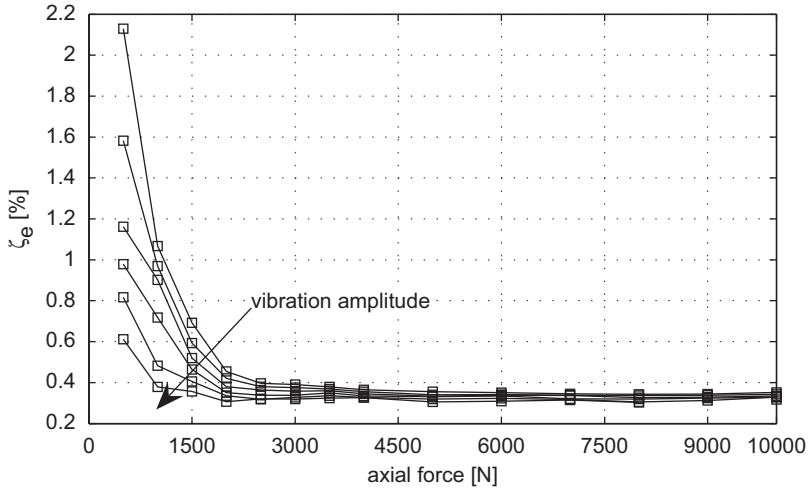

Fig. 16. Asymptotic evolution of the equivalent damping coefficient with increasing prestress.

evolution should also exists in the case of the assemblage with direct contact owing to a presumable local distribution of the interfacial pressure around the bolt axis. Such a localised pressure should also posses a limited perimeter beyond which the pressure vanishes. Therefore, when the continuing increase of vibration amplitude would deploy the friction area beyond this perimeter, the dissipation by friction would no longer increase. In order to verify this hypothesis, an experiment with a sufficiently strong excitation deploying the friction area over such a perimeter would have to be done. Unfortunately, the used electromagnetic shaker was not sufficiently powerful to allow such an excitation.

Besides qualitative changes in damping variations with respect to the prestress, one can also observe important quantitative damping changes when decreasing the prestress. In the case of assemblage w0, an increase of damping as

large as 500 percent was observed upon a prestress decrease from 10 000 to 500 N. As the friction between two beams is strongly conditioned by the applied prestress, those results proves that the frictional joints may provide a high passive damping capacity when the relative motion between substructures is not fully restricted.

Finally, an asymptotic damping stabilisation due to increasing prestress was identified as in the case of the damped eigenfrequency. Fig. 16 shows that when the prestress grows up the equivalent damping asymptotically tends to a same value for any applied vibration amplitude. In other words, the damping is getting linear upon increasing prestress owing to a restricted nonlinear slip damping.

5. Conclusions

The aim of this paper was to analyse the influence of frictional joints and their functional parameters on the global dynamic behaviour of built-up structures. For such a purpose an experimental study was carried out on a simple built-up structure consisting of two bolted beams designed so that the prestress and the interface area could be modified. To characterise its presumably nonlinear dynamic behaviour, the equivalent modal parameters were chosen. The identification of equivalent modal parameters was performed by a new experimental method developed under the assumptions of linear substructures and non-coupled quasilinear eigenmodes. The method is based on the use of the wavelet transform applied on the free-decay response. This method was used in the experiment for analysing the global dynamic behaviour of the studied assembled structure with regard to the functional parameters of the frictional joint represented by the prestress and the interface area. The results and main conclusions of the experiment may be summarised as follows:

- the frictional joint affects the dynamic behaviour of the whole structure only within a limited range of bolt axial forces and vibration amplitudes;
- the frictional joint influences only negligibly the eigenmode linearity at all applied prestresses and vibration amplitudes;
- at low bolt axial forces (up to 2000 N), the frictional joint gives rise to an important slip damping resulting in nonlinear amplitude dependent equivalent modal parameters;
- the equivalent modal parameters tend to stabilise at constant amplitude independent values when increasing the bolt axial force beyond a limit value;
- the equivalent eigenfrequency shows a linearly decreasing tendency with increasing amplitude at low bolt axial forces;
- at low bolt axial forces, the equivalent damping is strongly dependent on the vibration amplitude, bolt axial forces and interface area;
- at important vibration amplitudes, the equivalent damping reaches extreme values that are several times higher compared to its stabilised amplitude independent value at high axial bolt forces;
- the extreme values of the equivalent damping increases substantially with increasing interface area.

The experiment confirmed that the frictional joints are main sources of energy dissipation in built-up structures when applied prestresses allow for a relative motion of substructures. Under those circumstances the studied structure showed a high passive damping capacity as large as 2.5 percent that was five times more than under highly tightened conditions. The experiment also proved that the friction is not restricted at a localised area around the bolt but it is extended to much larger interface area. Hence, the passive damping capacity may be considerably increased by extending the interface area.

References

[1] E.E. Ungar, Energy dissipation at structural joints; mechanisms and magnitude, Air Force Flight Dynamics Laboratory, Wright-Pattersons Air Force Base, OH, USA, 1964.
[2] L. Gaul, R. Nitsche, The role of friction in mechanical joints, *Applied Mechanics Reviews* 54 (2) (2001) 93–106.
[3] E.E. Ungar, The status of engineering knowledge concerning the damping of built-up structures, *Journal of Sound and Vibration* 26 (1) (1973) 141–154.
[4] L.E. Goodman, A review of progress in analysis of interfacial slip damping, *Structural Damping*, American Society of Mechanical Engineers, 1959, pp. 35–48.
[5] L.E. Goodman, J.H. Klumpp, *Analysis of Slip Damping with Reference to Turbine-blade Vibration*, ASME Applied Mechanics Division, vol. 23, 1956, pp. 421–429.
[6] T.H.H. Pian, *Structural Damping of a Simple Built-up Beam with Riveted Joints in Bending*, ASME Applied Mechanics Division, Vol. 24, 1957, pp. 35–38.
[7] M. Masuko, Y. Ito, K. Yoshida, Theoretical analysis for damping ratio of a jointed cantibeam, *Bulletin of the JSME* 16 (1973) 1421–1432.
[8] L. Gaul, J. Lenz, Nonlinear dynamics of structures assembled by bolted joints, *Acta Mechanica* 125 (1–4) (1997) 169–181.
[9] Y. Song, C.J. Hartwigsen, D.M. McFarland, A.F. Vakakis, Simulation of dynamics of beam structures with bolted joints using adjusted Iwan beam elements, *Journal of Sound and Vibration* 273 (2004) 249–276.
[10] D.J. Segalman, An initial overview of Iwan modelling for mechanical joints, Sandia Report SAND2001-0811, Sandia National Laboratories, New Mexico and Livermore, CA, USA, 2001.
[11] Y. Ren, C.F. Beards, Identification of joint properties of a structure using FRF data, *Journal of Sound and Vibration* 186 (4) (1995) 567–587.
[12] K.Y. Sanliturk, D.J. Ewins, Modelling two-dimensional friction contact and its application using harmonic balance method, *Journal of Sound and Vibration* 193 (1996) 511–523.
[13] J.V. Ferreira, Dynamic Response Analysis of Structures with Nonlinear Components, Department of Mechanical Engineering, Imperial College of Science, Technology and Medicine, London, UK, 1998.

[14] H.R.E. Siller, Nonlinear Modal Analysis, Methods for Engineering Structures, Department of Mechanical Engineering, Imperial College of Science, Technology and Medicine, London, UK, 2004.
[15] A.H. Nayfeh, *Perturbation Methods*, Wiley, New York, 1973.
[16] M. Feldman, Non-linear system vibration analysis using Hilbert transform—part 1: free vibration analysis method FREEVIB, *Mechanical Systems and Signal Processing* 8 (2) (1994) 119–127.
[17] C.J. Hartwigsen, Y. Song, D.M. McFarland, L.A. Bergman, A.F. Vakakis, Experimental study of non-linear effects in a typical shear lap joint configuration, *Journal of Sound and Vibration* 277 (2004) 327–351.
[18] J.P. Kahane, P.G. Lemariée-Rieusset, *Séeries de Fourier et Ondelettes*, Cassini, Paris, 1998 ISBN 284225001X.
[19] B. Torréesani, Ondelettes, Analyse Temps-Fréequence et Signaux Non-Stationnaires, Lecture Notes, 1997.
[20] W.J. Staszewski, Identification of damping in MDOF systems using time-scale decomposition, *Journal of Sound and Vibration* 203 (2) (1997) 283–305.
[21] J. Lardies, S. Gouttebroze, Identification of modal parameters using the wavelet transform, *International Journal of Mechanical Sciences* 44 (2002) 2263–2283.
[22] T.-P. Le, P. Argoul, Continuous wavelet transform for modal identification using free decay response, *Journal of Sound and Vibration* 277 (2004) 73–100.
[23] M. Ruzzene, A. Fasana, L. Garibaldi, B. Piombo, Natural frequencies and damping identification using wavelet transform: application to real data, *Mechanical Systems and Signal Processing* 11 (2) (1997) 207–218.
[24] P. Argoul, T.-P. Le, Instantaneous indicators of structural behaviour based on the continuous Cauchy wavelet analysis, *Mechanical Systems and Signal Processing* 17 (1) (2003) 243–250.
[25] R. Ghanem, F. Romeo, A wavelet-based approach for model and parameter identification of non-linear systems, *International Journal of Non-Linear Mechanics* 36 (5) (2001) 835–859.